Redox Biology 57 (2022) 102490

Contents lists available at ScienceDirect

Redox Biology

journal homepage: www.elsevier.com/locate/redox

Seizures, ataxia and parvalbumin-expressing interneurons respond to selenium supply in *Selenop*-deficient mice

Ulrich Schweizer [a,*], Eva K. Wirth [b], Thomas Klopstock [c,d,e], Sabine M. Hölter [f,g], Lore Becker [f], Jackob Moskovitz [h], Tilman Grune [i,j,k,m], Helmut Fuchs [f], Valerie Gailus-Durner [f], Martin Hrabe de Angelis [f,l,m], Josef Köhrle [b], Lutz Schomburg [b]

[a] *Institut für Biochemie und Molekularbiologie, Uniklinikum Bonn, Rheinische Friedrich-Wilhelms-Universität Bonn, Bonn, Germany*
[b] *Institut für Experimentelle Endokrinologie, Charité-Universitätsmedizin Berlin, Berlin, Germany*
[c] *Friedrich-Baur-Institute, Department of Neurology, University Hospital, Ludwig Maximilian University of Munich, Ziemssenstraße 1a, 80336, Munich, Germany*
[d] *German Center for Neurodegenerative Diseases (DZNE), Munich, Germany*
[e] *Munich Cluster for Systems Neurology (SyNergy), Munich, Germany*
[f] *Institute of Experimental Genetics, German Mouse Clinic, Helmholtz Zentrum München, German Research Center for Environmental Health (GmbH), Neuherberg, Germany*
[g] *Institute of Developmental Genetics, Helmholtz Zentrum München, German Research Center for Environmental Health, Neuherberg, Germany*
[h] *Department of Pharmacology & Toxicology, University of Kansas, Lawrence, KS, USA*
[i] *Department of Molecular Toxicology, German Institute of Human Nutrition Potsdam-Rehbruecke (DIfE), 14558, Nuthetal, Germany*
[j] *German Center for Cardiovascular Research (DZHK), 10117, Berlin, Germany*
[k] *Department of Physiological Chemistry, Faculty of Chemistry, University of Vienna, 1090, Vienna, Austria*
[l] *Experimental Genetics, TUM School of Life Sciences, Technische Universität München, Alte Akademie 8, 85354, Freising, Germany*
[m] *German Center for Diabetes Research (DZD), Ingolstaedter Landstraße. 1, 85764, Neuherberg, Germany*

ARTICLE INFO

Keywords:
Epilepsy
PVALB
Selenoprotein
Brain
Dystonia

ABSTRACT

Mice with constitutive disruption of the *Selenop* gene have been key to delineate the importance of selenoproteins in neurobiology. However, the phenotype of this mouse model is exquisitely dependent on selenium supply and timing of selenium supplementation. Combining biochemical, histological, and behavioral methods, we tested the hypothesis that parvalbumin-expressing interneurons in the primary somatosensory cortex and hippocampus depend on dietary selenium availability in *Selenop*$^{-/-}$ mice. *Selenop*-deficient mice kept on adequate selenium diet (0.15 mg/kg, i.e. the recommended dietary allowance, RDA) developed ataxia, tremor, and hyperexcitability between the age of 4–5 weeks. Video-electroencephalography demonstrated epileptic seizures in *Selenop*$^{-/-}$ mice fed the RDA diet, while *Selenop* $^{\pm}$ heterozygous mice behaved normally. Both neurological phenotypes, hyperexcitability/seizures and ataxia/dystonia were successfully prevented by selenium supplementation from birth or transgenic expression of human SELENOP under a hepatocyte-specific promoter. Selenium supplementation with 10 μM selenite in the drinking water on top of the RDA diet increased the activity of glutathione peroxidase in the brains of *Selenop*$^{-/-}$ mice to control levels. The effects of selenium supplementation on the neurological phenotypes were dose- and time-dependent. Selenium supplementation after weaning was apparently too late to prevent ataxia/dystonia, while selenium withdrawal from rescued *Selenop*$^{-/-}$ mice eventually resulted in ataxia. We conclude that SELENOP expression is essential for preserving interneuron survival under limiting Se supply, while SELENOP appears dispensable under sufficiently high Se status.

1. Introduction

Selenoproteins are proteins containing the rare amino acid selenocysteine (Sec) [1]. The human and mouse genomes contain 25 and 24 genes encoding selenoproteins, respectively [2]. Co-translational incorporation of Sec requires several *cis*- and *trans*-acting factors, including selenocysteine insertion sequence (SECIS)-binding protein 2 (SECISBP2; [3]) and a specific elongation factor, EEFSEC [4], which

* Corresponding author. Uniklinikum Bonn, Rheinische Friedrich-Wilhelms-Universität Bonn, Institut für Biochemie und Molekularbiologie, Nussallee 11, 3115, Bonn, Germany.
E-mail address: ulrich.schweizer@uni-bonn.de (U. Schweizer).

https://doi.org/10.1016/j.redox.2022.102490
Received 22 August 2022; Received in revised form 19 September 2022; Accepted 22 September 2022
Available online 24 September 2022

cooperate to recruit Sec-tRNA^{Sec} to the ribosome [1,5].

The notion that the trace element selenium (Se) is essential for the mammalian brain became apparent only upon genetic inactivation of selenoprotein P (SELENOP) in mice [6,7], because otherwise brain Se levels were protected by preferential Se transport to the brain at the cost of the rest of the organism [8]. SELENOP is a plasma selenoprotein containing several Sec that is made in liver, but also expressed in several other organs [9]. Inactivation of the *Selenop* gene in mice significantly reduced Se content and selenoprotein activities in the brain and caused neurological phenotypes [6,7,10,11]. Subsequently, LRP8 and LRP2 were identified as SELENOP receptors preferentially taking up SELENOP into target organs like brain, kidney, and testes [12–15]. These and other studies arrived at a model for Se transport in mammals that places synthesis and secretion of SELENOP from the liver into blood in the center of Se transport [16]. The brain and the testes are most protected from dietary Se restriction, because the liver maintains SELENOP secretion and the target organs expressing the SELENOP receptor with the highest affinity, LRP8, will continue to take up circulating SELENOP to cover the Se requirements. SELENOP biosynthesis within the brain helps to fix Se within the brain, a process referred to as the SELENOP cycle [15,17,18].

A practical limitation for the study of Se in the brain using *Selenop*$^{-/-}$ mice was the phenotypic spectrum of knockout mice that was exquisitely sensitive to dietary Se levels of the mice. When raised on a Se-deficient diet (i.e. 0.06 mg/kg Se), *Selenop*$^{-/-}$ suffered from massive neurodegeneration [19,20]. In contrast, when kept on a diet containing supra-nutritional Se, *Selenop*$^{-/-}$ mice showed little phenotype [21], and mice in the initial descriptions had an intermediate phenotype [6,7,10,11].

Because the *Selenop*$^{-/-}$ model was difficult to handle, and because there was still the possibility that the neurological phenotype might be secondary to any other pathology in constitutive *Selenop*-knockout mice, we specifically targeted selenoprotein expression in neurons: Neuron-specific inactivation of tRNA^{Sec} lead to massive neurodegeneration in preweaning mice suggesting that selenoproteins are indeed essential for neurons [22,23]. We subsequently found that these mice showed a seizure-like phenotype that could be substantiated in electrophysiological studies, and lacked the development of the most abundant class of GABAergic interneurons in cortex and hippocampus, the parvalbumin (PVALB) expressing neurons [22]. These PVALB + neurons are important to limit network activity. Hence, their loss was associated with seizure-like episodes in neuron-specific *Secisbp2* knockout mice [24]. Neuron-specific inactivation of *Gpx4* alone replicated the phenotype of mice lacking all neuronal selenoproteins demonstrating that lack of GPX4 caused the lack of PVALB + interneurons [22,25]. These findings were in line with the finding that limiting the availability of glutathione (GSH) in *Gclm*$^{-/-}$ mice likewise reduced the number of PVALB + interneurons in the ventral hippocampus [26]. Interestingly, PVALB + interneurons were shown to express the SELENOP receptor LRP8 [27]. Accordingly, *Lrp8*$^{-/-}$ share many phenotypic similarities with *Selenop*$^{-/-}$ mice [28].

The aim of this study was to characterize the neurological phenotypes of *Selenop*$^{-/-}$ mice in more detail and to explore the potential and limits of Se supplementation of *Selenop*$^{-/-}$ mice. To this end, we fed the mice a diet containing the recommended dietary allowance (RDA) of Se [29] and supplemented Se as sodium selenite via the drinking water during specific periods of development. In addition, in order to avoid potentially toxic effects of selenite, we carefully titrated the Se supplementation to a level which restored normal GPX1 activity in the brains of *Selenop*$^{-/-}$ mice. We report here reduced densities of PVALB+ interneurons in somatosensory cortex and hippocampus, seizure-like electroencephalographic recordings, and an in-depth description of the neurological phenotype including tremor and ataxia/dystonia in *Selenop*$^{-/-}$ mice. Mice with the neurological phenotype display increased astrogliosis in the cerebral cortex. We show that all these phenotypes can be prevented by Se supplementation after birth and before weaning or by transgenic expression of a liver-specific SELENOP transgene.

2. Materials and methods

Mouse husbandry and selenium supplementation. *Selenop*-deficient mice were described elsewhere [7] and were kept on a defined diet containing 0.15–0.16 mg/kg Se (C1045, Altromin, Lage, Germany). Selenium supplementation was provided via the drinking water at 1, 10, and 100 μM sodium selenite [11] or with a diet containing 0.24–0.26 mg/kg Se (1314 M, Altromin, Lage, Germany). Mice carrying a human *SELENOP* transgene regulated under control of a hepatocyte-specific transthyretin promoter were described before [18]. If not otherwise indicated, male and female mice were included in all analyses and *Selenop*$^{+/+}$ and *Selenop*$^{-/-}$ mice were littermates from heterozygous matings. At the GMC mice were housed in individually ventilated caging (IVC) systems (VentiRack Bioscreen TM, Biozone, Margate, UK) according to German laws.

In-house score. In order to independently record the hyperexcitability/seizures and the movement disorder of *Selenop*$^{-/-}$ mice, we established a simple scheme in which both aspects were scored separately. Normal behavior was rated “0”. Hyperexcitability/irritability was rated “1”. Additional periods of inactivity/freezing or undirected grooming were rated “2”. Grand mal seizures were rated “3”. Regarding the movement phenotype, a wide, “shuffling” gait was rated “1”. If the animal’s ability to move was significantly impaired, the animal was rated “2”. Severe problems to move or inability to support the body were rated “3”. “0.5” could be added to any score, if the observer wanted to note an intermediate phenotype. This score was particularly useful in predicting the survival of *Selenop*$^{-/-}$ mice, since animals rated “3 + 3” were likely to die within one or two days and were thus immediately euthanized.

Fixed bar test. The animal was placed on a 1 cm wide, 50 cm long wooden bar that was elevated 30 cm above a cage with wood-chips bedding. The animal was placed on the rod and the time was noted until the *Selenop*$^{-/-}$ mouse fell from the rod. Wild-type and heterozygous mice were able to balance more than 120 s on the bar.

Rotarod. The movement disorder was quantified using the rotarod device (Ugo Basile, Comerio, Italy) essentially as described [11,17]. Briefly, after 3 min of accommodation in an arena around the running rotarod device, the mice were placed on the rotating rod (4 r.p.m.) for additional 2–3 min and immediately put back, if they fell off. Then the animals were tested five times in acceleration mode (linear acceleration of 4–40 r.p.m. within 5 min) with at least 3 min rest between trials. Since *Selenop*$^{-/-}$ mice are hyperexcitable, careful accommodation of the animals to the apparatus was mandatory.

Western Blot: Protein extracts were prepared from brain tissue powder by addition of lysis buffer (50 mM Tris pH 7.5, 150 mM NaCl, 1 mM EDTA, 0.1% Igepal and protease inhibitor cocktail (Sigma)), followed by sonication and centrifugation at 4 °C for 15 min at 15,000 RPM. Extracts were electrophoresed on NuPage 10% polyacrylamide gels, transferred to PVDF membranes and immunoblotted with antibodies against GPX1 (1:1000 dilution, Abcam, Cambridge, UK), GPX4 (1:2000), MSRB1 (1:1000), SELENOT (1:400), SELENOM (1:1000), and SELENOF (1:1000). GPX4, MSRB1, SELENOT, SELENOS, and SELENOM, antibodies were kindly provided by Dr. Vadim Gladyshev, Harvard University. The SELENON antiserum 168 was kindly provided by Dr. Alain Lescure, Université Strasbourg. Anti-rabbit-HRP conjugated secondary antibody (Sigma) (1:30000) was used in all Western blots. Membranes were washed with 0.1% TBS-T, incubated in SuperSignal West Dura Extended Duration Substrate (Pierce) and exposed to X-ray film.

Enzyme activities: GPX activity was measured as described [7]. MSRA + B: MSR activity was measured by using 20 mM DTT, 200 μM Dabsyl-*R*- or *S*-MetO (the *R* or *S* form of MetO is for monitoring the MSRB or MSRA activity, respectively), and tissue extract supernatant. After 30 min of incubation at 37 °C, the separation and quantitation of the Dabsyl-Met product were performed by using an HPLC method, as described [30].

Reduced glutathione (GSH) and oxidized glutathione (GSSG) determination: For analysis of GSH and GSSG concentrations in red blood cells, plasma was removed and cells were diluted to equal volumes by 0.9% NaCl solution. Samples were drawn with ice cold metaphosphoric acid and kept at 4 °C. Samples were centrifuged for 10 min at 1200 g. Supernatants were collected and separated into two aliquots for the GSH and GSSG measurements [31]. GSH was assayed by means of Ellman's reagent (DTNB). GSSG was determined fluorimetrically after addition of *o*-phthaldialdehyde. GSH autoxidation was prevented by addition of 50 mM *N*-ethylmaleimide (NEM). The glutathione ratio was calculated as the share of total glutathione bound in the oxidized form [2GSSG x (GSH $+2GSSG)^{-1}$].

Malondialdehyde measurement: MDA was determined according to Wong et al. [32] with modifications of Sommerburg et al. [33] as the thiobarbituric acid (TBA) derivative. Phosphoric acid (440 mM), sample or MDA standard, and TBA solution (42 mM) were incubated at 100 °C for 60 min and then the samples and standards were cooled on ice. To neutralize the phosphoric acid and to precipitate the proteins before the sample was injected into the HPLC system, the samples and standards were diluted 1:1 (v:v) with NaOH (0.1 M) in methanol. Afterwards, all samples were centrifuged at 10,000 g for 2 min. Aliquots of the derivatized samples were injected into the reversed phase HPLC and separated by isocratic elution with phosphate buffer (50 mM, pH 6.8) containing 40% (v/v) methanol. TBA–MDA complex was detected by means of fluorescence using an excitation wavelength of 525 nm and emission of 550 nm.

Protein carbonyl determination: For determination of PCO groups, the method of Voss et al. was used [34]. After determination of the protein concentration, the samples were diluted to the same concentration of protein (1 mg/ml) and derivatized with DNPH solution. Sample loading, washing of ELISA plates and development was performed as described by Ref. [34]. The absorbance of the derivatized samples at 492 nm was measured and the concentration of protein bound carbonyls was calculated by standards of oxidized bovine serum albumin (BSA). Blanks of PBS without protein were subtracted from standards and samples absorbencies. Oxidized BSA was prepared by modifying solved BSA with hypochlorite. The carbonyl content of the oxidized BSA was determined according to Buss et al. [35]. Reduced BSA was obtained as described by Buss et al.

Histology: Brains of five weeks old *Selenop*$^{-/-}$ mice and litter mates were immersion-fixed in 4% paraformaldehyde/0.1 M sodium phosphate buffer, pH 7.4 (PB). After cryoprotection in 30% sucrose in PB, brains were frozen on dry ice and stored at −80 °C. Sections of 25–35 μm thickness were cut on a cryostat. Nissl staining was done as described [36]. Immunostaining on free-floating sections was performed with the following antibodies: rabbit anti-calbindin (1:5000; SWANT, Bellinzona, Switzerland), rabbit anti-parvalbumin (1:5000; SWANT), rabbit anti-calretinin (1:1000; SWANT), mouse anti-glutamic acid decarboxylase (GAD67; 1:5000, Chemicon), rabbit anti-NPY (1:1000; ThermoFisher), rabbit anti-somatostatin (SST; 1:1000, SWANT), mouse anti-glial acidic fibrillary protein (GFAP; Sigma). Immunoreactivity was visualized with horseradish peroxidase using the Vectastain reagents (Vector, Burlingame, VT, USA) and the M.O.M. Kit (Vector) with diaminobenzidine (DAKO) as substrate.

Counting of neurons. PVALB+ interneurons were counted in a rectangular area marked in photomicrographs of the primary somatosensory cortex (S1BF) and expressed as neurons per mm^2. About 2000 neurons were counted per condition. In the hippocampus, immunoreactive interneurons were counted in each designated cell layer in the ventral hippocampus. 6–7 coronal sections were evaluated per genotype and antibody as indicated.

SHIRPA protocol. A modified version of the SHIRPA (SmithKline Beecham, MRC Harwell, Imperial College, the Royal London hospital phenotype assessment) protocol was used to test 23 parameters that contribute to an overall assessment of muscle, lower motor neuron, spinocerebellar, sensory and autonomic function as described [37].

Grip strength. Forelimb muscle strength was measured by a grip strength meter (TSE; Bad Homburg, Germany). Five trials within 1 min were performed for each mouse. The repeated measurements were analyzed by a linear mixed effects model [37].

Modified Hole Board. Spontaneous locomotor and exploratory activity as well as social affinity, anxiety and object recognition in a novel environment were assessed using the modified Hole Board test carried out as previously described [38,39]. One 5-min trial was performed for each mouse.

Electroencephalography (EEG). A transmitter was placed subcutaneously in the lower lateral trunk with the leads routed subcutaneously to an incision accessing the cranium. Trepanations (1 mm deep in the skull) were done with a microdrill on each side of the midline and 1 mm anterior of the lambda fissure. Microscrews placed in the drill holes directly above the dura and acted as electrodes for the EEG lead which is wrapped round the screws. EEG recordings were collected with an RPC-1 telemetry receiver (Data Science International), which was placed beneath the mouse cage at a sampling rate of 250 Hz. With the DSI PhysioTel® telemetry system, mice were monitored while moving freely in their cages. A miniaturized implant transmits the digitized data via radio frequency signals to a receiver. The data were collected with the Dataquest® software.

Spectral analysis of EEGs. Spectral analysis was performed using 24 consecutive 10-sec EEG samples. Each 10-sec period was divided into 8 overlapping segments of 2.56 s. After band-pass filtering (1–40 Hz), elimination of linear trends and tapering, each segment was submitted to Fast Fourier transformation (FFT) resulting in the distribution of spectral power values in [μV^2] with a frequency resolution of 0.488 Hz. The consecutive spectral evaluation of EEG signals was performed as described [40]. For feature extraction, the peak frequency of the power spectra and the steepness of the peak were calculated from each normalized power spectrum and averaged over 24 periods.

Statistics. If not otherwise stated, data of male and female mice was analyzed separately comparing mutant and control data using a Student's *t*-test. Sex differences within the mutant or the control group also were determined with a *t*-test. Tables summarizing the data show mean values ± the standard error of the mean (SEM). The Chi-Squared test was applied for categorial data. Figures were prepared and significance calculated with GraphPad Prism Software (San Diego, USA).

Approvals. Landesamt für Gesundheit und Soziales Berlin, G0008/08, District government of Upper Bavaria, 112-01.

3. Results

3.1. Characterization of Selenop-deficient mice fed an adequate selenium diet

When mice deficient in *Selenop* were fed a diet containing the recommended dietary allowance (RDA, 0.15 mg/kg) of Se, they developed a recognizable neurological phenotype between the fourth and fifth postnatal week. This phenotype consisted of a wide and dystonic gait, tremor, hyperexcitability, and even seizures (Supplemental Video S1). These phenotypes were observed on mixed, 129Ola/Hsd, and C57Bl/6J genetic backgrounds. Since there were no apparent differences in the neurological phenotypes among *Selenop*$^{-/-}$ mice on different genetic backgrounds, the 129Ola/Hsd line was discontinued and biochemical and histological measurements were obtained exclusively from mice on the C57Bl/6J genetic background.

Supplementary data related to this article can be found at https://doi.org/10.1016/j.redox.2022.102490.

Reduced expression of selenoproteins in brains of mice deficient in *Selenop* have been described several times, but seizures were described only in *Selenop*$^{-/-}$ mice with the additional inactivation of *Scly* [41]. Western blot analysis on postnatal day 35 (P35) confirmed reduced selenoprotein expression in the brains of *Selenop*$^{-/-}$ mice fed the RDA diet (Fig. 1a). While decreased GPX1 activities in *Selenop*$^{-/-}$ mice have

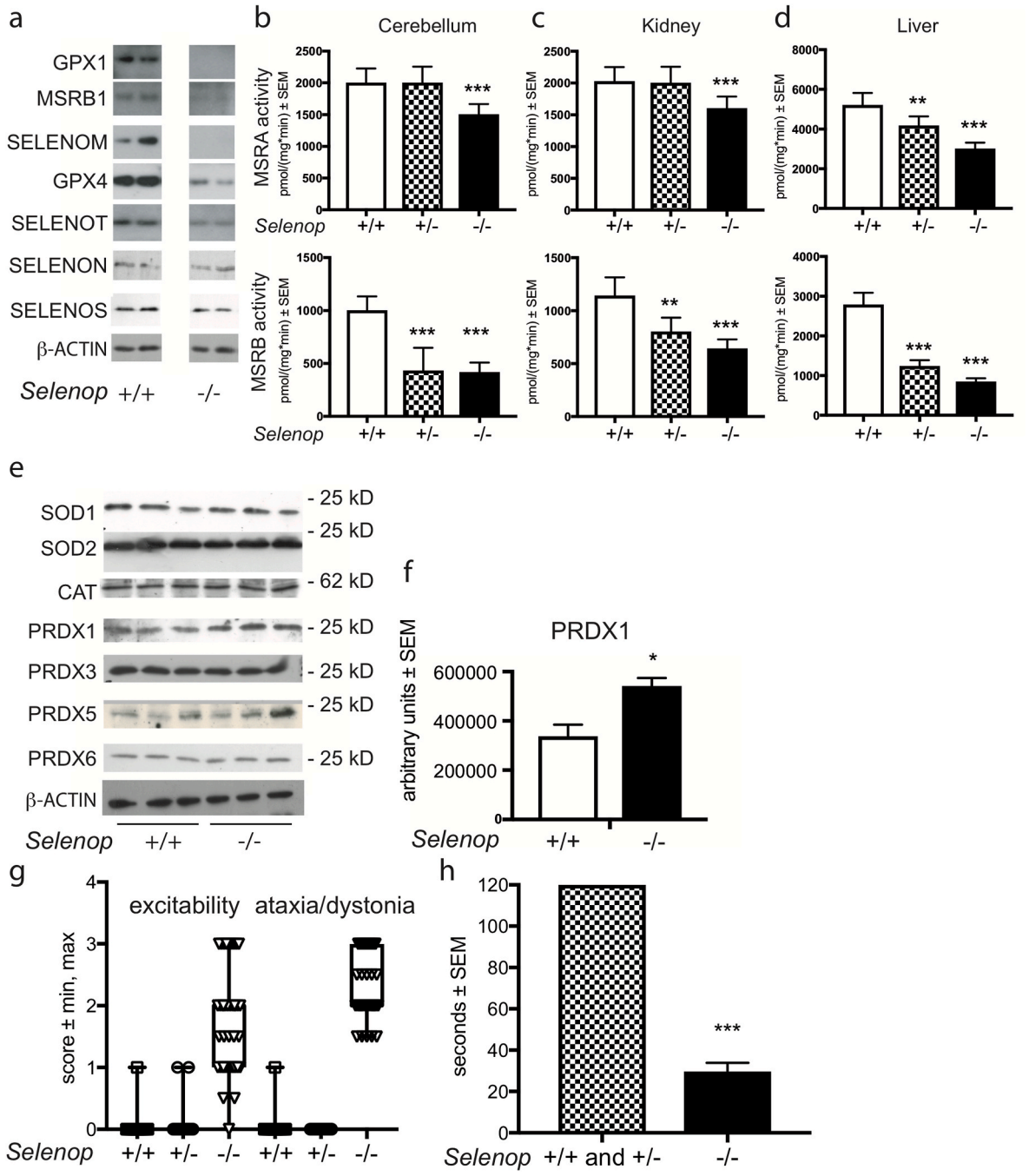

Fig. 1. Characterization of *Selenop*-deficient mice fed an adequate selenium diet. (**a**) Cortical selenoprotein expression is reduced in *Selenop*-deficient mice Western blot analysis of individual mice. (**b**) Methionine-sulfoxide-reductase A and B activities in cerebella of six mice per genotype. (**c**) Methionine-sulfoxide-reductase A and B activities in kidneys of six mice per genotype. (**d**) Methionine-sulfoxide-reductase A and B activities in livers of six mice per genotype. (**e**) Western blot analysis of non-selenium containing antioxidant enzymes in cerebral cortex. Three individual mice per genotype were analyzed at P35. (**f**) Densitometric quantification shows induced expression of PRDX1 in *Selenop*$^{-/-}$ mice. (**g**) Scores for excitability and ataxia/dystonia are higher in *Selenop*$^{-/-}$ mice. N = 28, 21, and 41 for *Selenop* +/+, +/−, and −/−, respectively. (**h**) Fixed bar test. In contrast to *Selenop*$^{+/+}$ and *Selenop*$^{+/-}$ mice, *Selenop*$^{-/-}$ mice are unable to stay on the fixed bar for 120 s (n = 7 for *Selenop*$^{-/-}$, n = 19 for controls). *p < 0.05, **p < 0.01, ***p < 0.001.

been described repeatedly, we show here reduced activities of the Se-dependent MSRB1 and its non-Se dependent isoenzyme MSRA in cerebellum, kidney, and liver (Fig. 1b–d). As expected, limited availability of Se reduced MSRB1 activity [30]. Interestingly, MSRA activities were also decreased, a finding reminiscent of reduced MSRB activities in *MsrA*$^{-/-}$ mice [30]. The remaining MSR activities are apparently still sufficient to keep changes in methionine-sulfoxides below detection limits in *Selenop*$^{-/-}$ mice (Table 1). These findings are in line with the genetic inactivation of *MsrB1*, which affected MSRA activity, but did not increase methionine-sulfoxide levels in brain [42]. We then assessed the expression of a number of anti-oxidant enzymes in the brain, but did not find any changes except for an induction of PRDX1 in *Selenop*$^{-/-}$ mice (Fig. 1e and f). Several biochemical markers of oxidative stress, including reduced and oxidized GSH, protein carbonylation, and malondialdehyde remained unchanged in *Selenop*$^{-/-}$ brains compared to controls (Table 1).

We wanted to obtain an easily applicable measure to relate the neurological phenotype of each individual *Selenop*$^{-/-}$ mouse with

Table 1
Biochemical markers of oxidative stress in brain.

Parameter	RDA diet			RDA plus 10 μM selenite in drinking water		
	Selenop$^{+/+}$	Selenop$^{+/-}$	Selenop$^{-/-}$	Selenop$^{+/+}$	Selenop$^{+/-}$	Selenop$^{-/-}$
Reduced glutathione (GSH) nmol/mg protein	4.36 ± 0.32	4.29 ± 0.30	4.42 ± 0.33	3.48 ± 0.15[b]	3.81 ± 0.55	3.51 ± 0.36[c]
Oxidized glutathione (GSSG) pmol/mg protein	85 ± 16	74 ± 13	75 ± 21	76 ± 10	75 ± 14	70 ± 9
Glutathione ratio (Q) (2GSSG/GSH+2xGSSG)	3.71 ± 0.55	3.36 ± 0.54	3.56 ± 0.58	4.15 ± 0.43	3.76 ± 0.41	3.81 ± 0.23
Protein carbonyls (CO) pmol/mg protein	5.8 ± 1.9	6.0 ± 1.3	6.7 ± 2.3	4.3 ± 1.9	4.7 ± 1.2	3.8 ± 1.3[c]
Malondialdehyde (MDA) nmol/mg protein	0.70 ± 0.10	0.82 ± 0.11	0.78 ± 0.13	0.51 ± 0.09[c]	0.73 ± 0.15	0.52 ± 0.13[c]
Methionine sulfoxides (%MetSO of total Met)	8 ± 1	8 ± 1	7 ± 1	9 ± 1	10 ± 1	11 ± 1

Data are from five-week-old animals (n = 6 for each group) and are shown as means ± SEM.
One-way ANOVA with Dunnett's multiple comparison test.
[b] Mean different from *Selenop*$^{+/+}$; no supplement.
[c] Mean different from *Selenop*$^{-/-}$; no supplement.

biochemical findings. To this end, we graded each animal according to "excitability" and "ataxia/dystonia" using an in-house score as explained in the methods section (Fig. 1g). This scoring was complemented by a more objective procedure, the fixed bar test. While control litter-mates passed the test by remaining on the fixed bar over 120 s, none of the *Selenop*$^{-/-}$ mice stayed more than 75 s on the bar (Fig. 1h). To us, their difficulty to remain on the 1 cm wide bar seemed to primarily depend on the dystonia of the hindlimbs.

In order to more comprehensively describe *Selenop*$^{-/-}$ mice and control littermates, 12 males (5 *Selenop*$^{-/-}$ and 7 controls) and 21 females (7 *Selenop*$^{-/-}$ and 14 controls) were subjected to a comprehensive phenotypic screen at the German Mouse Clinic (GMC, [37]). In the neurology screen, several abnormalities were noted in *Selenop*$^{-/-}$ mice, including tremor, impaired reflexes, reduced grip strength, inability to perform the wire manoeuvre, and increased lactate levels (Table 2). In the behavioral screen, mice showed reduced locomotion and rearing, as well as abnormal object recognition test results (Table 3). Generally, male mice appeared to present a stronger phenotype than female mice as previously reported by Raman et al. [21].

3.2. Reduced numbers of PVALB-expressing interneurons in hippocampus and cortex

We have previously shown that PVALB expressing GABAergic interneuron numbers are reduced in mice with impaired expression of selenoproteins in the brain [22,24,25,43]. We, therefore, stained ventral hippocampal sections for several interneuron markers and quantified their numbers in the various cell layers of the hippocampal formation. While Nissl staining did not reveal pathological changes, the number of GAD67 cells was clearly reduced in several layers of the hippocampus (Fig. 2a and b). PVALB+ interneurons representing the majority of GABAergic interneurons were reduced in number by up to 50% depending on the hippocampal cell layer (Fig. 2a and b). In addition, we found a reduced number of somatostatin (SST)+ interneurons in the *stratum oriens* in CA1 and CA3. The number of neurons expressing neuropeptide Y (NPY) was only reduced in the *stratum radiatum* in the CA3 region. In contrast, we observed overexpression of NPY along the mossy fiber tract (Fig. 2a, arrows). This finding is indicative of epileptic activity in the hippocampus and thought to represent a physiological reaction to limit excitation in the hippocampus [44].

When we stained brain sections from *Selenop*$^{-/-}$ mice for PVALB, we found a significant reduction of the number of PVALB+ neurons in the primary somatosensory cortex at P35, which was not apparent at P16 (Fig. 3a). P16 is the age at which the number of PVALB expressing neurons reaches its maximum in this brain area in mice (Supplementary Fig. 1). Feeding the mice with a Se-supplemented diet at 0.24 mg/kg ("high Se") rescued PVALB+ interneuron numbers in the somatosensory cortex (Fig. 3b). This Se content in the diet is below the level at which Byrns et al. found unaltered PVALB+ interneuron numbers in *Selenop*$^{-/-}$ mice [41].

Table 2
Primary Neurology screen at the German Mouse Clinic (GMC).

Parameter	male		female		*Selenop*$^{+/+}$ *vs.* *Selenop*$^{-/-}$ *(P value)*	
	+/+	−/−	+/+	−/−	male	female
Tremor (present)	0/7	5/5	0/14	4/7	0.001	0.00001
Locomotor activity	17 ± 1.4	8 ± 2 .8	12 ± 2.1	9 ± 1.5	0.01	0.05
Tail elevation[a] (dragging)	0/7	5/5	1/14	3/7	0.001	n.s.
Touch escape (no response)	0/7	3/5	0/14	2/7	0.004	0.053
Limb grasping (present)	0/7	4/5	0/14	0/7	0.001	n.s.
Grip strength (none or slight grip)	0/7	4/5	0/14	2/7	0.001	0.014
Wire manoeuvre (falls off immediately)	0/7	5/5	1/14	5/7	0.03	0.001
Righting reflex (lands on side or back)	0/7	5/5	0/14	3/7	0.001	0.001
Contact righting reflex (absent)	0/7	5/5	0/14	4/7	0.001	0.001
Negative geotaxis (turns and climbs)	7/7	0/5	14/14	4/7	0.001	0.01
Lactate levels	6 ± 0.4	7.1 ± 0.8	5.9 ± 0.3	8.3 ± 0.8	n.s.	0.03

Data are from ten-week-old animals and are shown as means ± SEM or number of animals/total number of animals; n.s. not significant; The Chi-Squared test was applied except for locomotor activity (means ± SEM; Kruskal-Wallis-test (S-PLUS, Insightful). *Selenop*$^{+/+}$ and *Selenop*$^{+/-}$ mice were not different and thus results from *Selenop*$^{-/-}$ mice are not reported.
[a] Some parameters, e.g. tail elevation, are seemingly in contradiction to observations made in 3–5 weeks old animals. However, since the more affected *Selenop*$^{-/-}$ mice died before reaching the GMC neurology screen, the data likely reflect the selection of less affected *Selenop*$^{-/-}$ mice for the GMC screen. Alternatively, it is possible that the mouse diet provided at the GMC during the initial screen contained more than adequate levels of Se (see Discussion section). The full list of results (12 tables) from the GMC behavior screen is available on request.

3.3. Effects of selenium supplementation on the movement disorder

We tried to rescue *Selenop*$^{-/-}$ mice maintained on the RDA diet by supplementation with sodium selenite in drinking water from conception. Supplementation with 1 μM Se was insufficient to fully rescue the movement coordination defect in *Selenop*$^{-/-}$ mice (Fig. 4a). Increasing the Se dose to 10 μM, completely normalized the rotarod performance of *Selenop*$^{-/-}$ mice compared to wild-type and heterozygous littermates (Fig. 4b). The same dose-response relationship and full rescue at 10 μM were apparent in the "excitability" and "ataxia/dystonia" scores (Fig. 4c), consistent with our earlier report using 100 μM Se

Table 3
Behavioral screen at the German Mouse Clinic (GMC).

Parameter	Selenop$^{+/+}$ (A)		Selenop$^{-/-}$ (B)		Ā B (P value)	
	Male (n = 7)	Female (n = 13)	Male (n = 5)	Female (n = 6)	male	female
Modified hole board test						
Line crossing (frequency)	121.71 ± 4.48	128.92 ± 4.55	60.20 ± 16.48	87.17 ± 18.48	<0.05	<0.05
Line crossing (latency)	0.94 ± 0.12	1.45 ± 0.37	63.60 ± 59.15	24.22 ± 22.56	<0.05	n.s.
Rearings in box (frequency)	29.43 ± 2.30	26.46 ± 1.20	5.60 ± 2.50	10.17 ± 3.26	<0.05	<0.05
Hole exploration (frequency)	34.71 ± 2.49	24.62 ± 1.15	6.60 ± 2.09	9.17 ± 3.34	<0.05	<0.05
Board entry (frequency)	12.86 ± 1.62	8.15 ± 0.90	2.20 ± 0.92	3.67 ± 2.17	<0.05	<0.05
Board entry (latency)	36.73 ± 11.19	74.01 ± 8.07	196.88 ± 42.27	187.92 ± 44.83	<0.05	<0.05
Board entry duration (% total duration)	11.29 ± 1.07	7.97 ± 0.57	4.43 ± 2.00	4.27 ± 1.71	<0.05	<0.05
Group contact (frequency)	9.86 ± 0.46	10.00 ± 0.98	3.40 ± 1.57	8.33 ± 0.92	<0.05	n.s.
Grooming (frequency)	1.14 ± 0.34	0.77 ± 0.20	0.20 ± 0.20	0.33 ± 0.21	<0.05	n.s.
Unfamiliar object exploration (frequency)	6.71 ± 1.32	4.46 ± 0.69	1.20 ± 0.37	1.83 ± 0.87	<0.05	<0.05
Familiar object exploration (frequency)	7.57 ± 0.90	7.15 ± 0.81	1.60 ± 0.51	2.67 ± 0.67	<0.05	<0.05
Video tracking results						
Distance moved (cm)	3412.51 ± 106.11	3359.06 ± 105.69	1701.64 ± 351.61	2324.51 ± 468.60	<0.05	<0.05
Mean velocity (cm/sec)	20.40 ± 0.45	20.96 ± 0.52	10.95 ± 2.12	13.69 ± 2.34	<0.05	<0.05
Turns (frequency)	1756.79 ± 41.77	1703.33 ± 31.32	1042.56 ± 173.48	1336.89 ± 216.45	<0.05	<0.05

Data are from 9-week-old animals and are shown as means ± SEM; n.s. not significant; *Selenop*$^{+/+}$ and *Selenop*$^{+/-}$ mice were not different and thus results from *Selenop*$^{+/-}$ mice are not reported. It is possible that the mouse diet provided at the GMC during the initial screen contained more than adequate levels of Se. For space limitations, more parameters from the GMC behavior screen are available upon request.

supplementation from conception [11].

We then asked, whether we could identify a time window during which Se supplementation needs to be present. When we commenced Se supplementation with 100 μM Se in drinking water at birth of the new litter, *Selenop*$^{-/-}$ pups were still fully rescued according to their rotarod performance (Fig. 4d), while the same supplementation was ineffective, when initiated from weaning on P21 (Fig. 4e).

Next, we wondered whether withdrawal of an effective selenite supplementation would ultimately lead to a deterioration of the neurological phenotype of *Selenop*$^{-/-}$ mice. Thus, mice were kept on the RDA diet and supplemented from birth with 100 μM Se in drinking water until the age of 8 weeks. Se supplementation was then discontinued and the movement phenotype was detecta ble 5 weeks after Se withdrawal (Fig. 4f). The same mice were followed until the age of 21 weeks (13 weeks of Se withdrawal) and the rotarod performance was similar as in *Selenop*$^{-/-}$ mice not rescued with Se (Fig. 4g). While these animals developed the movement phenotype, we did not observe hyperexcitability or seizures. By variation of the Se supplementation period, we established that the seizure phenotype of *Selenop*$^{-/-}$ mice was caused by cerebral Se deficiency during the first three weeks of life (Fig. 4h). Whether it is developmental or degenerative cannot be concluded based on the experiments reported here. It may be degenerative, since *Selenop*$^{-/-}$*/Scly*$^{-/-}$ mice developed seizures and loss of PVALB+ neurons at several months of age even when supplemented with increased dietary Se [41]. The movement phenotype, in our experiments, clearly has a degenerative component, as it occurred with a delay after Se withdrawal.

3.4. Effect of selenium supplementation on selenoenzyme activities in the brain

We then asked how the effective Se supplementation restored cerebral selenoenzyme activities. GPX1 activity was fully rescued in *Selenop*$^{-/-}$ brains by 10 μM Se supplementation on top of the RDA diet (Fig. 5a). Increased Se availability even increased cerebral GPX1 activities above normal in *Selenop*$^{+/+}$ and *Selenop*$^{+/-}$ mice. Moreover, Se supplementation normalized MSRB1 activity in *Selenop*$^{+/-}$ mice, and increased MSRB1 activity in *Selenop*$^{-/-}$ mice, although not up to control levels (Fig. 5b). As described in *MsrB1*-deficient mice, MSRA, which is not a selenoenzyme, was also reduced in *Selenop*$^{-/-}$ mice and depended on MSRB activity (Fig. 5c) [42]. Taken together, these results suggest that the phenotypic rescue at 10 μM Se supplementation correlates with restoration of Se availability in the brains of *Selenop*$^{-/-}$ mice.

3.5. Epilepsy in Selenop$^{-/-}$ mice can be prevented by selenium supplementation or hepatocyte-specific expression of a SELENOP transgene

In order to better asses the seizure phenotype of *Selenop*$^{-/-}$ mice maintained on the RDA diet, video-electroencephalography (EEG) was performed (Fig. 6a). Spectral analysis showed a clear difference between *Selenop*$^{-/-}$ mice as compared to wild-type and heterozygous mice. The 15 *Selenop*$^{-/-}$ mice showed a spike-like EEG activity of 7–9 Hz, while the 26 wild-type and 9 heterozygous mice showed a lower frequency activity (Supplementary Fig. 2). Thus, the automatic EEG showed a high discriminating power. Increasing brain Se levels by feeding the mice with a diet containing 0.24 mg/kg Se ("high Se") prevented development of seizures (Fig. 6a). A more physiological route of increasing cerebral Se levels, i.e. by transgenic expression of human *SELENOP* under control of a hepatocyte-specific promoter [18], also prevented seizure activity in *Selenop*$^{-/-}$ mice, even when maintained on the RDA diet (Fig. 6a). The transgene did not affect the *Selenop*$^{+/+}$ mice. In line with the observation that Se supplementation or *SELENOP* expression ameliorated the neurological phenotype and prevented seizure activity, PVALB-expressing interneurons were preserved in the primary somatosensory cortex (Fig. 6b). Astrogliosis, i.e. the enhanced expression of GFAP by astrocytes, was widespread in the brains of *Selenop*$^{-/-}$ mice maintained on the RDA diet and indicated brain pathology in these mice. Astrogliosis was prevented in *Selenop*$^{-/-}$ mice fed the high Se diet. Even if fed the RDA diet, *Selenop*$^{-/-}$ mice could be rescued, when carrying one allele of a hepatocyte-specific *SELENOP* transgene (Fig. 6b). Taken together, these results suggest that seizure activity in *Selenop*$^{-/-}$ mice correlates with reduced cortical PVALB expressing interneuron numbers and increased GFAP expression. These phenotypes can be rescued by increased dietary Se or transgenic expression of SELENOP in liver. Thus, SELENOP is required to provide bioavailable Se to the brain, where PVALB+ interneurons depend on it. This concept is consistent with the expression of the SELENOP-receptor, ApoER2/LRP8, on PVALB+ GABAergic interneurons [27].

4. Discussion

Selenop$^{-/-}$ mice are the first experimental animal model that allowed to substantially decrease cerebral Se levels and study the neurological consequences of selenoprotein deficiency in the mammalian brain [6,7]. Yet, the neurological phenotypes were found very sensitive to dietary Se levels. Standard breeding diets often contain supra-nutritional levels of

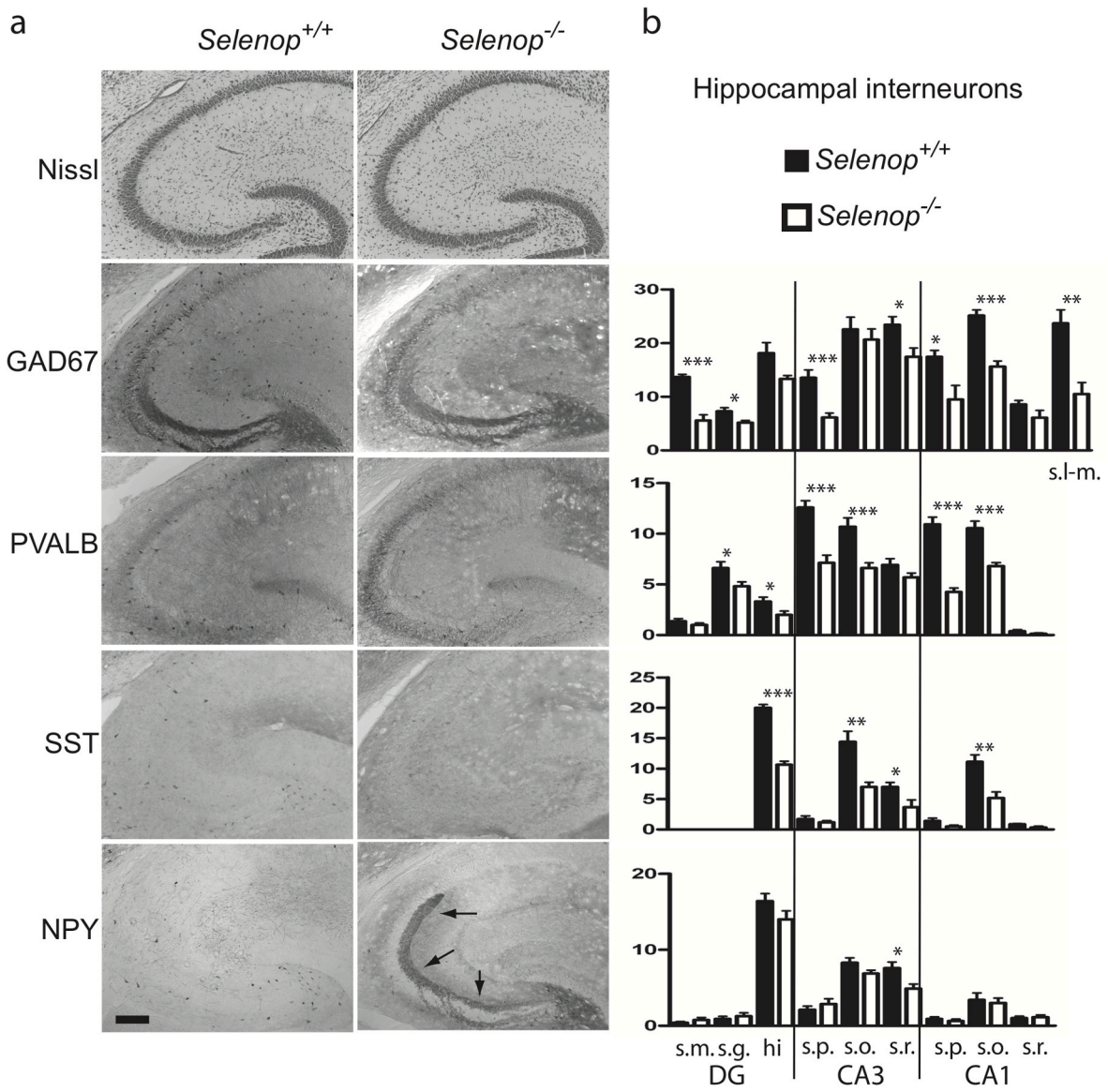

Fig. 2. Loss of GABAergic marker expression in the ventral hippocampus of *Selenop*-deficient mice. (**a**) Histological staining of ventral hippocampus from mice on P35. Arrows indicate the increased NPY immunoreactivity along the mossy fiber tract. (**b**) Quantitative analysis of marker-positive interneuron numbers in different cell layers of the hippocampus. 6 to 7 sections of ventral hippocampus were analyzed from 3 animals of each genotype. DG, dentate gyrus; CA1, CA3, ammon's horn region 1 or 3; s.m., stratum moleculare; s.g., stratum granulare; hi, hilus; s.p. stratum pyramidale; s.o., stratum oriens; s.r. stratum radiatum; s.l-m., stratum lacunosum moleculare. *p < 0.05, **p < 0.01, ***p < 0.001 calculated by two-tailed Student's *t*-test; scale bar 200 μm.

selenite (e.g. 0.25 mg/kg Se), which is not a normal dietary source of Se for mice or men, and is able to reach the brain bypassing SELENOP-dependent routes [20,41]. Other researchers have kept *Selenop*$^{-/-}$ on a Se-deficient *Torula* yeast diet (0.06–0.08 mg/kg Se), thus potentiating their phenotype, or on a supra-nutritional Se diet thus mitigating their phenotypes [20]. So, what should we refer to when describing the phenotype of *Selenop*$^{-/-}$ mice? What could be "standard conditions"? We decided here to explore the neurological phenotype of *Selenop*$^{-/-}$ mice that were fed a diet containing exactly the RDA of Se for wild-type rats which is generally believed to apply to mice, too (0.15 mg/kg; [29]).

The phenotype of *Selenop*$^{-/-}$ mice fed a diet containing the RDA of Se is dominated by two aspects: a movement disorder that has features of ataxia and dystonia, and a hyperexcitability that leads to seizures of either the grand mal type or absence seizures with or without automatisms of chewing or self-grooming behavior. In addition, tremor was often noted by different observers.

In this work, we show the first EEG analyses of *Selenop*$^{-/-}$ mice, which objectively support the earlier observations of seizures in these mice (Fig. 6). Moreover, unbiased EEG analysis confirms that *Selenop*$^{\pm}$ mice are indistinguishable from *Selenop*$^{+/+}$ mice. Dietary supplementation at 0.25 mg/kg from birth rescued the hyperexcitability phenotype of *Selenop*$^{-/-}$ mice in our experiments as well as in others [20,41]. The mice that were analyzed in the neurology screen at the German Mouse Clinic (GMC) were raised on RDA diet until transfer to the GMC. There, they were maintained on a standard diet at elevated (0.25 mg/kg Se). Thus, in hindsight, the *Selenop*$^{-/-}$ mice that survived and made it into the EEG analysis at ten weeks of age were rescued by a diet containing more Se than the RDA. Audiogenic seizure activity was reported in *Selenop*$^{-/-}$ mice fed 0.25 mg/kg Se, but only when the mice were, in addition, genetically deficient in selenocysteine lyase, SCLY [41]. This observation suggests that Se liberated by SCLY from Sec contributes to the available Se pool in the brain. Consistent with these findings, hippocampal synaptic function was moderately altered in *Selenop*$^{-/-}$ mice, albeit these mice were rescued with a diet containing excessive Se (1 mg/kg as selenite) [45].

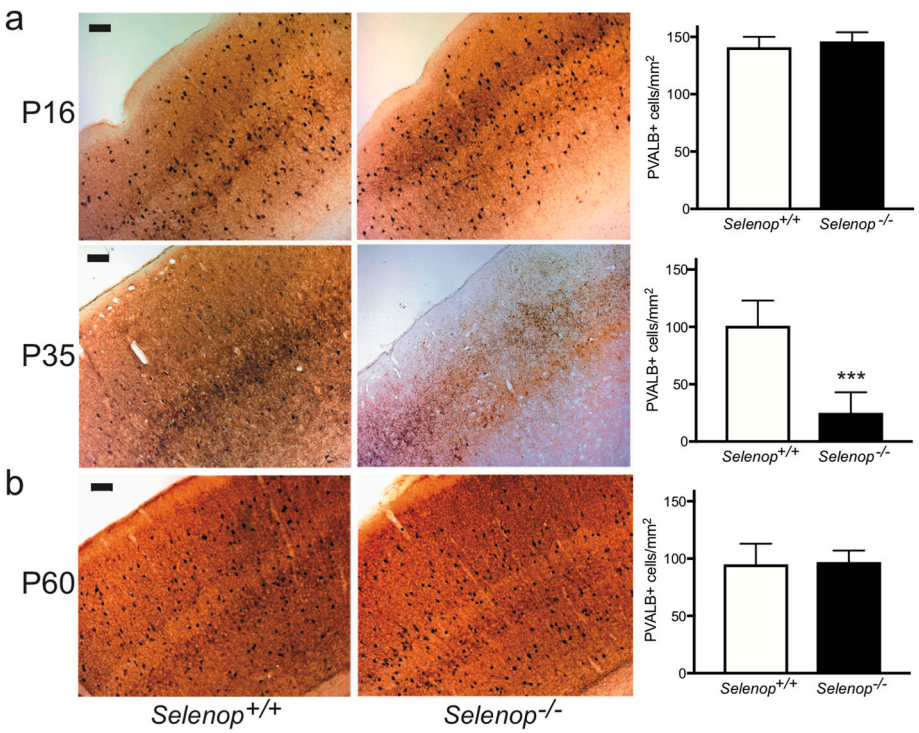

Fig. 3. Histological staining of PVALB+ interneurons in the primary somatosensory cortex. (**a**) Mice were fed an adequate Se diet (0.15 mg/kg). While the density of PVALB+ neurons was unchanged in *Selenop*$^{-/-}$ mice on postnatal day (P)16, interneuron density was significantly decreased in *Selenop*$^{-/-}$ mice on P35. More than 2000 neurons were counted per time point and group. ***p < 0.001 calculated by two-tailed Student's *t*-test. (**b**) When mice were fed a diet containing 0.24 mg/kg Se, interneuron density remained normal in *Selenop*$^{-/-}$ mice on P60.

The movement coordination defect of *Selenop*$^{-/-}$ mice was reported several times [10,11,17,18,21,41,45], but mostly the mice were fed either with a Se-deficient or a supra-nutritional Se diet. Sometimes the diets were switched around weaning, further complicating evaluation. Here, we kept the breeding females and their litters on the Se-adequate RDA diet and explored the timing and dose-response of Se-supplementation via the drinking water (Fig. 4). We chose this route, because selenite supplementation provided via the drinking water to breastfeeding mothers was known to be passed to the suckling offspring [11,17]. Careful investigation of the timing of supplementation was important, because Se supplementation from weaning was too late to rescue the movement phenotype (Fig. 4e), while Se supplementation of the mother from birth was still effective. We also showed that a Se supplementation of 10 μM selenite in drinking water on top of the RDA diet completely rescued cerebral GPX1 activity, although this supplementation was not entirely sufficient to normalize cerebral MSRB activity (Fig. 5). Yet, this concentration was sufficient to correct the excitability and ataxia/dystonia scores (Fig. 4c) and the stride length of *Selenop*$^{-/-}$ mice [17], while 1 μM selenite was not enough to achieve either. Based on our observations of *Selenop*$^{-/-}$ mice kept on different defined and closely monitored diets, we suppose now that the diet which we had used in our first studies did not contain the 0.24 mg/kg Se printed on the label, but was most probably very close to the RDA level of 0.15 mg/kg [7,11]. In fact, a prospective study of the Se content in "standard breeding diet" used in our animal facility revealed that the diet ranged between 0.16 and 0.28 mg/kg Se oscillating around the expected 0.25 mg/kg with the seasons of the year.

The results from the primary neurology and behavior screens at the GMC are consistent with studies by Pitts and Raman [21,27]. The latter studies used a standard lab chow containing 0.25 mg/kg Se until weaning and then switched the diets to Se-deficient (0.08 mg/kg) or supra-nutritional (1 mg/kg) Se. We bred the mice on a diet close to the RDA before we shipped them to the German Mouse Clinic, where they received standard lab chow (presumably containing around 0.25 mg/kg Se). In hindsight, this may be the reason why we initially lost *Selenop*$^{-/-}$ mice around shipping (5–6 weeks), but then the surviving *Selenop*$^{-/-}$ mice stabilized and passed through the screens.

The difficulties to control dietary Se levels in the *Selenop*$^{-/-}$ mice prompted us to choose an orthogonal approach and genetically inactivate or diminish selenoprotein biosynthesis in neurons. A hypomorphic tRNA^{Sec} allele, *Trsp*^{Staf}, lead to hyperexcitability in mutant mice along with astrocytosis and reduced numbers of PVALB+ interneurons [43]. Genetic deletion of tRNA^{Sec} in neurons caused a hyperexcitable phenotype and pre-weaning death of mutant mice [22] which was similar to neuron-specific inactivation of *Gpx4* [25]. These mouse models also have reduced numbers of PVALB + interneurons in the cortex and hippocampus [22,25]. Neuron-specific inactivation of *Secisbp2* also reduced cortical PVALB+ interneuron numbers and caused a movement disorder and seizure-like fits [24]. Pitts et al. reported normal numbers of PVALB + interneurons in the hippocampus of *Selenop*$^{-/-}$ when fed a 0.25 mg/kg Se-supplemented diet [27]. However, they found a reduction of PVALB+ neurons in the inferior colliculus, a region previously identified as a site of neuronal damage in *Selenop*$^{-/-}$ mice fed a low Se diet [28]. GABAergic interneurons are important to limit excitation in neuronal networks. Their largest subgroup in the cortex and hippocampus expressed PVALB. Other subtypes express the co-transmitters NPY and SST. Here, we show that the number of PVALB+, SST+, and NPY+ interneurons is reduced in several cellular layers of the ventral hippocampus of *Selenop*$^{-/-}$ mice when fed with the Se-adequate 0.15 mg/kg Se diet. We also show that the number of PVALB+ neurons in the primary somatosensory cortex first reaches normal levels (on P16) and the numbers are decreased afterwards when the seizures occur (P35). Consistent with Byrns' results, we found normal PVALB + neuron density in the cortex, when the *Selenop*$^{-/-}$ mice were fed a 0.24 mg/kg Se-supplemented diet. Our findings suggest a degenerative loss of PVALB+ interneurons, which is consistent with their sensitivity to oxidative stress [26,46] and their expression of the SELENOP-receptor, LRP8 [27]. LRP8 is, however, not the only SELENOP-receptor in the brain, although it is specifically important for PVALB+ interneurons. Cerebral GPX1 activity was reduced in *Lrp2*-deficient mice fed a 0.15 mg/kg Se RDA diet [13]. Feeding *Lrp2*$^{-/-}$ mice a low Se diet caused a movement coordination defect, albeit without reducing PVALB+ neuron numbers [13]. Along these lines, feeding *Lrp8*$^{-/-}$ mice the RDA diet did not lead to a movement coordination defect at P35 as in *Selenop*$^{-/-}$ mice

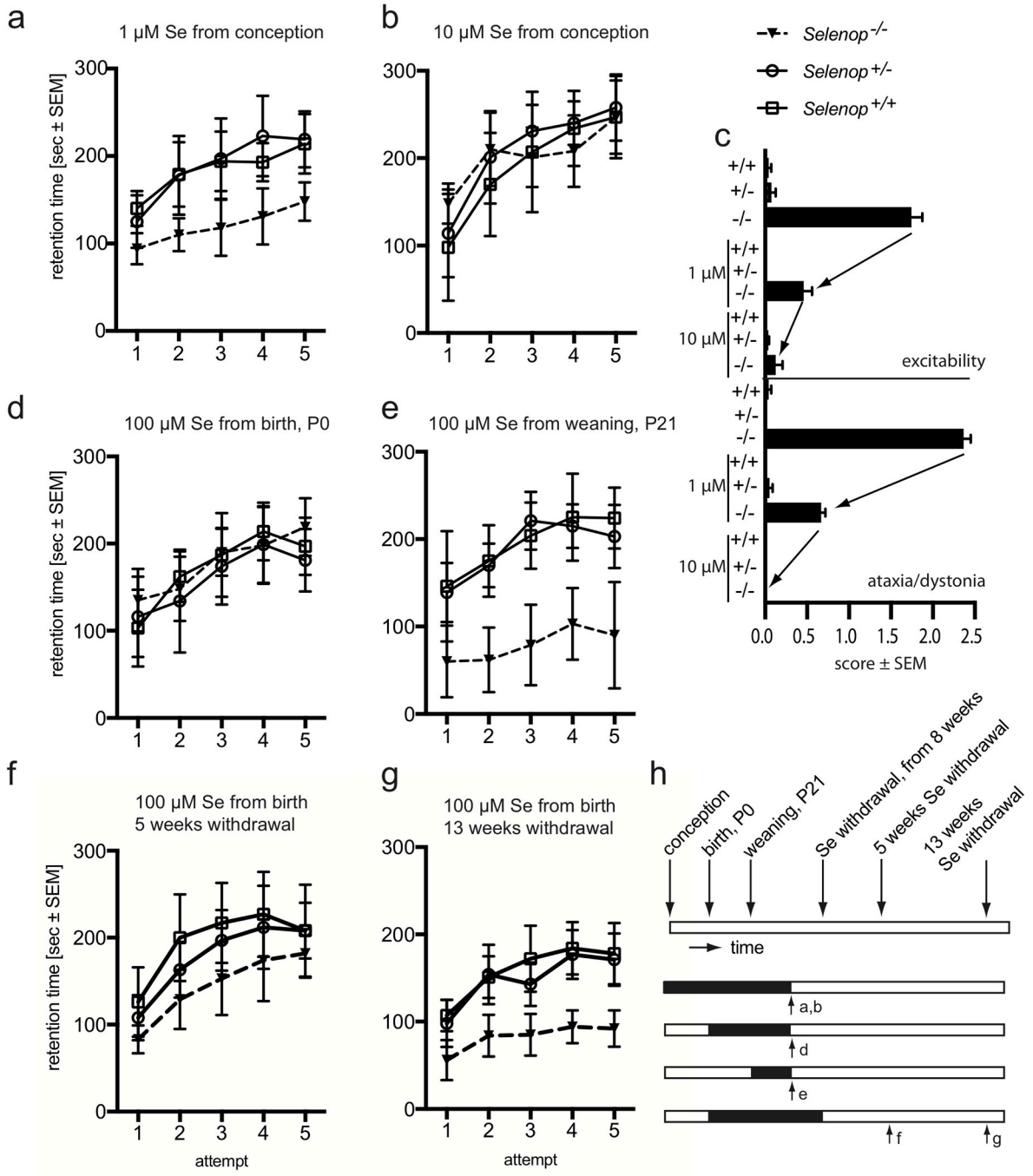

Fig. 4. Effect of selenium supplementation on neurological phenotypes in *Selenop*$^{-/-}$ mice. (**a**) Rotarod analysis of mice supplemented with 1 µM of selenite in drinking water from the day of conception. 5 *Selenop*$^{+/+}$, 14 *Selenop*$^{+/-}$, 7 *Selenop*$^{-/-}$ mice. (**b**) Rotarod analysis of mice supplemented with 10 µM of selenite in drinking water from the day of conception. 5 *Selenop*$^{+/+}$, 9 *Selenop*$^{+/-}$, 5 *Selenop*$^{-/-}$ mice. (**c**) Dose-dependent effect of Se supplementation on "excitability" and "ataxia/dystonia" scores. (**d**) Rotarod analysis of mice supplemented with 100 µM of selenite in drinking water from the day of birth. 8 *Selenop*$^{+/+}$, 11 *Selenop*$^{+/-}$, 6 *Selenop*$^{-/-}$ mice. (**e**) Rotarod analysis of mice supplemented with 100 µM of selenite in drinking water from the day of weaning. 6 *Selenop*$^{+/+}$, 13 *Selenop*$^{+/-}$, 10 *Selenop*$^{-/-}$ mice. (**f**) Rotarod analysis of mice supplemented with 100 µM of selenite in drinking water from the day of birth until 8 weeks of age. At the day of analysis, Se supplementation was withdrawn for 5 weeks. 8 *Selenop*$^{+/+}$, 11 *Selenop*$^{+/-}$, 6 *Selenop*$^{-/-}$ mice. (**g**) Same mice as in (f), but after 13 weeks of Se withdrawal. (**h**) Schematic summary of Se supplementation regimens in this figure. Arrows indicate time of rotarod analysis, periods of Se supplementation are indicated in black. Indices refer to the respective panel in this figure.

(Supplementary Fig. 3). Thus, feeding a strictly adequate RDA diet helped to reveal that at least two endocytic receptors cooperate to bring SELENOP into the brain and provide Se to target cells.

Neurodegeneration in *Selenop*$^{-/-}$ mice is consistent with increased expression of GFAP by astrocytes, which was found early-on [20,22,25,43]. We show here that Se supplementation or expression of a hepatic *SELENOP*-transgene can prevent the astrogliosis along with PVALB+ interneuron loss and seizures. Neurodegeneration, however, occurs beyond PVALB+ neurons as shown by Nissl and silver staining [19,20,22,28,41]. Increased GFAP expression and reduced PVALB+ expression was also demonstrated in *Selenop*$^{-/-}$ mice and neuron-specific *Secisbp2* knockout mice [24,41]. A recent study showed that SELENOP plays a role in hippocampal neurogenesis supporting proliferation of precursors and differentiation of neurons [47]. To our knowledge, these processes

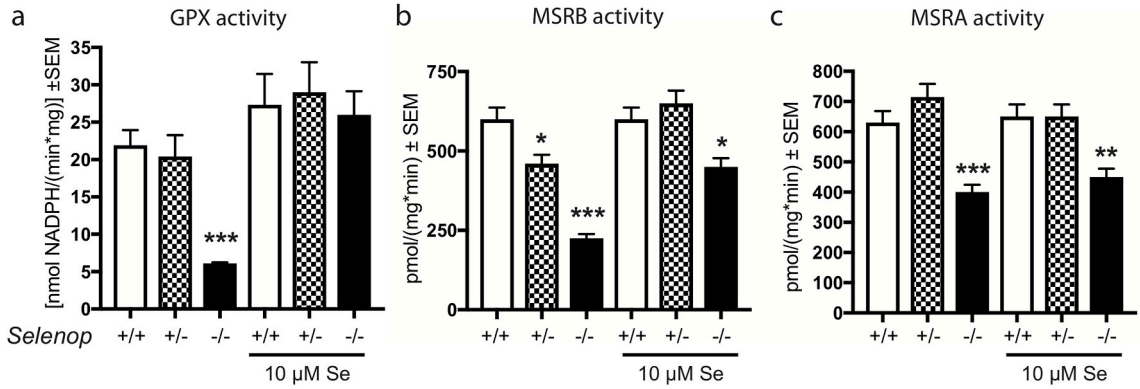

Fig. 5. Selenoenzyme activities in forebrains on postnatal day 35. Effect of selenium supplementation (sodium selenite, 10 µM) supplementation in drinking water from conception. (**a**) GPX1 activity. (**b**) MSRB activity. (**c**) MSRA activity. Results represent average values ± standard error of the mean (SEM) of 6 individual mice per group. *p < 0.05, **p < 0.01, ***p < 0.001 calculated by two-tailed Student's *t*-test vs. *Selenop*$^{+/+}$.

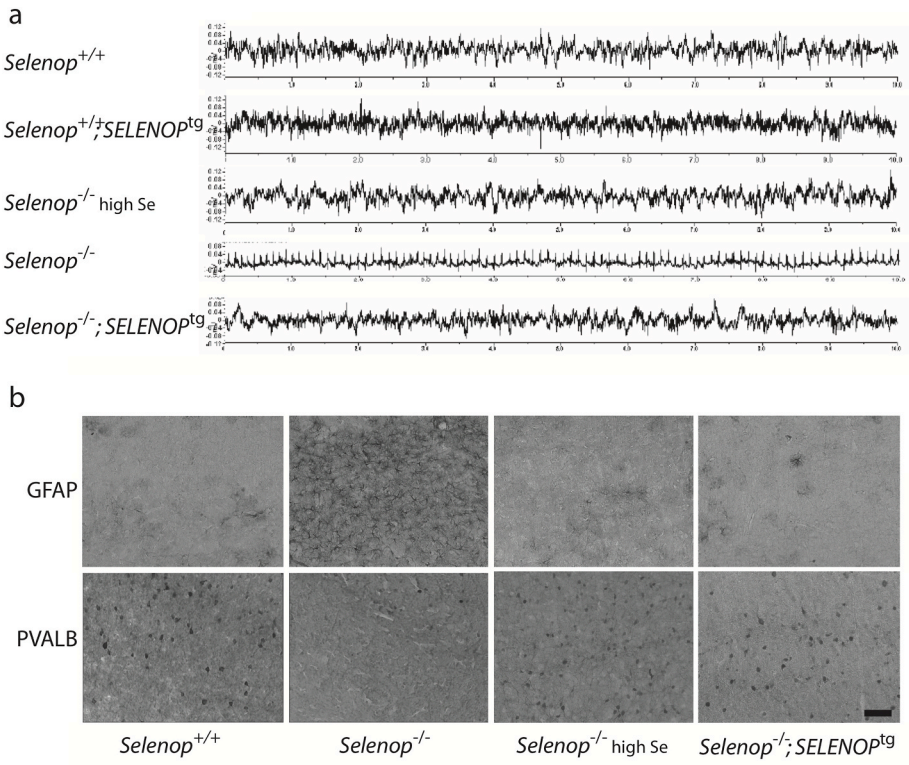

Fig. 6. Phenotypic rescue of *Selenop*$^{-/-}$ mice through selenium supplementation or hepatocyte-specific SELENOP expression. (**a**) Traces of electroencephalography (EEG) measurements. Mice were maintained on a diet containing adequate selenium levels (0.15 mg/kg) or were supplemented with additional selenium "high Se" (0.24 mg/kg); representative data of 3–6 individual mice, (**b**) Immunohistochemistry against glial fibrillary acidic protein (GFAP) and parvalbumin (PVALB) in primary somatosensory cortex. *SELENOP*^{tg} denotes one copy of the hepatocyte-specific human *SELENOP* transgene. Scale bar 100 µm.

have not been systematically studied in mouse models deficient in selenoprotein biosynthesis. Neuron-specific inactivation of tRNA^{Sec} demonstrated decreased postnatal granule cell proliferation leading to cerebellar hypoplasia, although the mechanisms were not investigated [23]. Inactivation of *Txnrd1* affected cerebellar development, but only in the neural, and not the neuronal, lineage [48]. This finding suggested that TXNRD1 is important for non-neuronal cells.

Recently, a deletion mutation of 17 kilobases comprising the entire genomic region of *SELENOP* was identified in Belgian shepherd dogs [49]. Homozygous dogs were affected with tremor, ataxia, increased muscle tone, and "episodic fits". The authors reported "stress dependent extensor muscle spasms", an observation that we occasionally made when handling *Selenop*$^{-/-}$ mice fed the RDA diet. Such stress dependent spasms were also observed in neuron-specific *Secisbp2* knockout mice [24]. Histopathological analysis of homozygous dogs showed cerebral and cerebellar atrophy, axonal degeneration, gliosis, and myelin loss [49]. With the exception of myelin loss these findings are the same as in *Selenop*$^{-/-}$ mice, if not supplemented with supra-physiological dietary Se. Like *Selenop*$^{-/-}$ mice fed an adequate Se diet, affected dogs developed the phenotype in the first weeks after birth. Only one, unrelated, dog with the same homozygous deletion reached ten years of age showing a similar phenotypic range among *SELENOP*-deficient dogs as in *Selenop*$^{-/-}$ mice fed different levels of Se.

Cerebral and cerebellar atrophy was the diagnosis of children affected by homozygous mutations in selenocysteine synthase, *SEPSECS* [50]. This condition independently demonstrated the importance of selenoprotein expression in the brain thereby suggesting that the phenotype of *Selenop*$^{-/-}$ mice is caused by decreased cerebral selenoprotein expression and not by any other hypothetical mechanism. Mice carrying the same missense mutation in *Sepsecs* died perinatally and had a deficiency of selenoprotein expression in the brain [51]. Most importantly, *Sepsecs*-mutant mice could be rescued with a Se-independent GPX4^{U46C} transgene [51,52]. That GPX4 is an essential selenoprotein in the brain is supported by the identification of patients with mutations

in *GPX4* who are affected by cerebral atrophy [53,54]. Two other selenoproteins are important for brain function in humans: thioredoxin reductase 1 (TXNRD1) and SELENOI. *TXNRD1* mutations were identified in patients with generalized epilepsy [55]. Mutations in *SELENOI* lead to complicated spastic paraplegia, a neurodegenerative condition that involves myelin loss [56,57].

5. Conclusions

We present the neurological phenotype of *Selenop*$^{-/-}$ mice fed an adequate Se diet that is based on the recommended dietary allowance for Se. We show that these knockout mice develop a severe neurological phenotype including tremor, ataxia/dystonia, and seizures that is correlated with a loss of interneurons in somatosensory cortex and hippocampus. Dogs with genetic deficiency of *SELENOP* show a very similar phenotype. Our description differs from other reports on *Selenop*$^{-/-}$ mice that were fed diets containing either unphysiologically low or supraphysiological high Se levels. We suggest from our own experience that dietary Se levels for animal models in Se research should be carefully adjusted, monitored and justified in order to gain full scientific advantage of the respective model.

Author contributions

Conceptualization, U.S. and L.S.; methodology, S.H., L.B., T.K.; investigation, E.K.W., U.S., J.M., T.G., W.T., L.B., S.H.; resources, M. HdA., J.K.; writing—original draft preparation, U.S.; writing—review and editing, S.H., T.K.; visualization, U.S., W.T.; supervision, V.G-D., H. F., T.K., J.K.; project administration, V.G-D., H.F.; funding acquisition, U.S., J.K., M.HdA. and L.S. All authors have read and agreed to the published version of the manuscript.

Funding

This research was funded by Deutsche Forschungsgemeinschaft DFG grant numbers Ko822/8, Scho849/1, Schw914/2, and Charité-Universitätsmedizin Berlin and by the German Federal Ministry of Education and Research (Infrafrontier grant 01KX1012). T.G.and L.S. were supported by FOR-2558 “TraceAge”.

Institutional review board statement

The animal study protocols were approved by the governmental authorities Landesamt für Gesundheit und Soziales Berlin, G0008/08, and District government of Upper Bavaria, 112-01.

Declaration of competing interest

L.S. holds shares of selenOmed GmbH, a company involved in Se status assessment. All other authors declare no conflict of interest. The funders had no role in the design of the study; in the collection, analyses, or interpretation of data; in the writing of the manuscript; or in the decision to publish the results.

Data availability

Data will be made available on request.

Acknowledgments

Invaluable technical assistance was provided by Vartitér Seher, Silke Kappler, Anja Fischbach, and Antje Kretschmer. Some data are part of SiJie Zhang’s Master thesis in Medical Neurosciences at Charité-Universitätsmedizin Berlin.

Appendix A. Supplementary data

Supplementary data to this article can be found online at https://doi.org/10.1016/j.redox.2022.102490.

References

[1] P.A. Tsuji, D. Santesmasses, B.J. Lee, V.N. Gladyshev, D.L. Hatfield, Historical roles of selenium and selenoproteins in health and development: the good, the Bad and the ugly, Int. J. Mol. Sci. 23 (2022) 5, https://doi.org/10.3390/ijms23010005.
[2] G.V. Kryukov, S. Castellano, S.V. Novoselov, A.V. Lobanov, O. Zehtab, R. Guigo, V. N. Gladyshev, Characterization of mammalian selenoproteomes, Science 300 (2003) 1439–1443, https://doi.org/10.1126/science.1083516 300/5624/1439 [pii].
[3] P.R. Copeland, J.E. Fletcher, B.A. Carlson, D.L. Hatfield, D.M. Driscoll, A novel RNA binding protein, SBP2, is required for the translation of mammalian selenoprotein mRNAs, EMBO J. 19 (2000) 306–314.
[4] D. Fagegaltier, N. Hubert, K. Yamada, T. Mizutani, P. Carbon, A. Krol, Characterization of mSelB, a novel mammalian elongation factor for selenoprotein translation, EMBO J. 19 (2000) 4796–4805.
[5] T. Hilal, B.Y. Killam, M. Grozdanović, M. Dobosz-Bartoszek, J. Loerke, J. Bürger, T. Mielke, P.R. Copeland, M. Simonović, C.M.T. Spahn, Structure of the mammalian ribosome as it decodes the selenocysteine UGA codon, Science 376 (2022) 1338–1343, https://doi.org/10.1126/science.abg3875.
[6] K.E. Hill, J. Zhou, W.J. McMahan, A.K. Motley, J.F. Atkins, R.F. Gesteland, R. F. Burk, Deletion of selenoprotein P alters distribution of selenium in the mouse, J. Biol. Chem. 278 (2003) 13640–13646.
[7] L. Schomburg, U. Schweizer, B. Holtmann, L. Flohé, M. Sendtner, J. Köhrle, Gene disruption discloses role of selenoprotein P in selenium delivery to target tissues, Biochem. J. 370 (2003) 397–402, https://doi.org/10.1042/BJ20021853 BJ20021853 [pii].
[8] U. Schweizer, M. Fabiano, Selenoproteins in brain development and function, Free Radic. Biol. Med. 190 (2022) 105–115, https://doi.org/10.1016/j.freeradbiomed.2022.07.022.
[9] K.E. Hill, R.S. Lloyd, J.G. Yang, R. Read, R.F. Burk, The cDNA for rat selenoprotein P contains 10 TGA codons in the open reading frame, J. Biol. Chem. 266 (1991) 10050–10053.
[10] K.E. Hill, J. Zhou, W.J. McMahan, A.K. Motley, R.F. Burk, Neurological dysfunction occurs in mice with targeted deletion of the selenoprotein p gene, J. Nutr. 134 (2004) 157–161.
[11] U. Schweizer, M. Michaelis, J. Köhrle, L. Schomburg, Efficient selenium transfer from mother to offspring in selenoprotein-P-deficient mice enables dose-dependent rescue of phenotypes associated with selenium deficiency, Biochem. J. 378 (2004) 21–26, https://doi.org/10.1042/BJ20031795 BJ20031795 [pii].
[12] G.E. Olson, V.P. Winfrey, S.K. Nagdas, K.E. Hill, R.F. Burk, Apolipoprotein E receptor-2 (ApoER2) mediates selenium uptake from selenoprotein P by the mouse testis, J. Biol. Chem. 282 (2007) 12290–12297.
[13] J. Chiu-Ugalde, F. Theilig, T. Behrends, J. Drebes, C. Sieland, P. Subbarayal, J. Köhrle, A. Hammes, L. Schomburg, U. Schweizer, Mutation of megalin leads to urinary loss of selenoprotein P and selenium deficiency in serum, liver, kidneys and brain, Biochem. J. 431 (2010) 103–111, https://doi.org/10.1042/BJ20100779.
[14] G.E. Olson, V.P. Winfrey, K.E. Hill, R.F. Burk, Megalin mediates selenoprotein P uptake by kidney proximal tubule epithelial cells, J. Biol. Chem. 283 (2008) 6854–6860.
[15] R.F. Burk, K.E. Hill, A.K. Motley, V.P. Winfrey, S. Kurokawa, S.L. Mitchell, W. Zhang, Selenoprotein P and apolipoprotein E receptor-2 interact at the blood-brain barrier and also within the brain to maintain an essential selenium pool that protects against neurodegeneration, Faseb. J. 28 (2014) 3579–3588, https://doi.org/10.1096/fj.14-252874.
[16] R.F. Burk, K.E. Hill, Regulation of selenium metabolism and transport, Annu. Rev. Nutr. 35 (2015) 109–134, https://doi.org/10.1146/annurev-nutr-071714-034250.
[17] U. Schweizer, F. Streckfuss, P. Pelt, B.A. Carlson, D.L. Hatfield, J. Köhrle, L. Schomburg, Hepatically derived selenoprotein P is a key factor for kidney but not for brain selenium supply, Biochem. J. 386 (2005) 221–226, https://doi.org/10.1042/BJ20041973.
[18] K. Renko, M. Werner, I. Renner-Muller, T.G. Cooper, C.H. Yeung, B. Hollenbach, M. Scharpf, J. Köhrle, L. Schomburg, U. Schweizer, Hepatic selenoprotein P (SePP) expression restores selenium transport and prevents infertility and motor-incoordination in Sepp-knockout mice, Biochem. J. 409 (2008) 741–749, https://doi.org/10.1042/BJ20071172.
[19] W.M. Valentine, K.E. Hill, L.M. Austin, H.L. Valentine, D. Goldowitz, R.F. Burk, Brainstem axonal degeneration in mice with deletion of selenoprotein p, Toxicol. Pathol. 33 (2005) 570–576.
[20] S.W. Caito, D. Milatovic, K.E. Hill, M. Aschner, R.F. Burk, W.M. Valentine, Progression of neurodegeneration and morphologic changes in the brains of juvenile mice with selenoprotein P deleted, Brain Res. 1398 (2011) 1–12, https://doi.org/10.1016/j.brainres.2011.04.046.
[21] A.V. Raman, M.W. Pitts, A. Seyedali, A.C. Hashimoto, L.A. Seale, F.P. Bellinger, M. J. Berry, Absence of selenoprotein P but not selenocysteine lyase results in severe neurological dysfunction, Gene Brain Behav. 11 (2012) 601–613, https://doi.org/10.1111/j.1601-183X.2012.00794.x.
[22] E.K. Wirth, M. Conrad, J. Winterer, C. Wozny, B.A. Carlson, S. Roth, D. Schmitz, G. W. Bornkamm, V. Coppola, L. Tessarollo, L. Schomburg, J. Köhrle, D.L. Hatfield, U. Schweizer, Neuronal selenoprotein expression is required for interneuron

development and prevents seizures and neurodegeneration, Faseb. J. 24 (2010) 844–852, https://doi.org/10.1096/fj.09-143974.
[23] E.K. Wirth, B.S. Bharathi, D. Hatfield, M. Conrad, M. Brielmeier, U. Schweizer, Cerebellar hypoplasia in mice lacking selenoprotein biosynthesis in neurons, Biol. Trace Elem. Res. 158 (2014) 203–210, https://doi.org/10.1007/s12011-014-9920-z.
[24] S. Seeher, B.A. Carlson, A.C. Miniard, E.K. Wirth, Y. Mahdi, D.L. Hatfield, D. M. Driscoll, U. Schweizer, Impaired selenoprotein expression in brain triggers striatal neuronal loss leading to co-ordination defects in mice, Biochem. J. 462 (2014) 67–75, https://doi.org/10.1042/BJ20140423.
[25] A. Seiler, M. Schneider, H. Forster, S. Roth, E.K. Wirth, C. Culmsee, N. Plesnila, E. Kremmer, O. Radmark, W. Wurst, G.W. Bornkamm, U. Schweizer, M. Conrad, Glutathione peroxidase 4 senses and translates oxidative stress into 12/15-lipoxygenase dependent- and AIF-mediated cell death, Cell Metabol. 8 (2008) 237–248, https://doi.org/10.1016/j.cmet.2008.07.005.
[26] P. Steullet, J.H. Cabungcal, A. Kulak, R. Kraftsik, Y. Chen, T.P. Dalton, M. Cuenod, K.Q. Do, Redox dysregulation affects the ventral but not dorsal hippocampus: impairment of parvalbumin neurons, gamma oscillations, and related behaviors, J. Neurosci. 30 (2010) 2547–2558.
[27] M.W. Pitts, A.V. Raman, A.C. Hashimoto, C. Todorovic, R.A. Nichols, M.J. Berry, Deletion of selenoprotein P results in impaired function of parvalbumin interneurons and alterations in fear learning and sensorimotor gating, Neuroscience 208 (2012) 58–68, https://doi.org/10.1016/j.neuroscience.2012.02.017.
[28] W.M. Valentine, T.W. Abel, K.E. Hill, L.M. Austin, R.F. Burk, Neurodegeneration in mice resulting from loss of functional selenoprotein P or its receptor apolipoprotein E receptor 2, J. Neuropathol. Exp. Neurol. 67 (2008) 68–77.
[29] P.G. Reeves, Components of the AIN-93 diets as improvements in the AIN-76a diet, J. Nutr. 127 (1997) 838S–841S, https://doi.org/10.1093/jn/127.5.838S.
[30] J. Moskovitz, E.R. Stadtman, Selenium-deficient diet enhances protein oxidation and affects methionine sulfoxide reductase (MsrB) protein level in certain mouse tissues, Proc. Natl. Acad. Sci. U. S. A. 100 (2003) 7486–7490.
[31] W.G. Siems, R. Brenke, O. Sommerburg, T. Grune, Improved antioxidative protection in winter swimmers, QJM 92 (1999) 193–198, https://doi.org/10.1093/qjmed/92.4.193.
[32] S.H. Wong, J.A. Knight, S.M. Hopfer, O. Zaharia, C.N. Leach, F.W. Sunderman, Lipoperoxides in plasma as measured by liquid-chromatographic separation of malondialdehyde-thiobarbituric acid adduct, Clin. Chem. 33 (1987) 214–220.
[33] O. Sommerburg, T. Grune, S. Klee, F.R. Ungemach, W.G. Siems, Formation of 4-hydroxynonenal and further aldehydic mediators of inflammation during bromotrichlorornethane treatment of rat liver cells, Mediat. Inflamm. 2 (1993) 27–31, https://doi.org/10.1155/S0962935193000031.
[34] P. Voss, L. Horakova, M. Jakstadt, D. Kiekebusch, T. Grune, Ferritin oxidation and proteasomal degradation: protection by antioxidants, Free Radic. Res. 40 (2006) 673–683, https://doi.org/10.1080/10715760500419357.
[35] H. Buss, T.P. Chan, K.B. Sluis, N.M. Domigan, C.C. Winterbourn, Protein carbonyl measurement by a sensitive ELISA method, Free Radic. Biol. Med. 23 (1997) 361–366, https://doi.org/10.1016/s0891-5849(97)00104-4.
[36] L. Schomburg, C. Riese, M. Michaelis, E. Griebert, M.O. Klein, R. Sapin, U. Schweizer, J. Köhrle, Synthesis and metabolism of thyroid hormones is preferentially maintained in selenium-deficient transgenic mice, Endocrinology 147 (2006) 1306–1313, https://doi.org/10.1210/en.2005-1089.
[37] I. Schneider, W.S. Tirsch, T. Faus-Kessler, L. Becker, E. Kling, R.L. Busse, A. Bender, B. Feddersen, J. Tritschler, H. Fuchs, V. Gailus-Durner, K.H. Englmeier, M.H. de Angelis, T. Klopstock, Systematic, standardized and comprehensive neurological phenotyping of inbred mice strains in the German Mouse Clinic, J. Neurosci. Methods 157 (2006) 82–90.
[38] M. Kallnik, R. Elvert, N. Ehrhardt, D. Kissling, E. Mahabir, G. Welzl, T. Faus-Kessler, M.H. de Angelis, W. Wurst, J. Schmidt, S.M. Hölter, Impact of IVC housing on emotionality and fear learning in male C3HeB/FeJ and C57BL/6J mice, Mamm. Genome 18 (2007) 173–186, https://doi.org/10.1007/s00335-007-9002-z.
[39] K.B. Zumbrennen-Bullough, L. Becker, L. Garrett, S.M. Hölter, J. Calzada-Wack, I. Mossbrugger, L. Quintanilla-Fend, I. Racz, B. Rathkolb, T. Klopstock, W. Wurst, A. Zimmer, E. Wolf, H. Fuchs, V. Gailus-Durner, M.H. de Angelis, S.J. Romney, E. A. Leibold, Abnormal brain iron metabolism in Irp2 deficient mice is associated with mild neurological and behavioral impairments, PLoS One 9 (2014), e98072, https://doi.org/10.1371/journal.pone.0098072.
[40] W. Tirsch, M. Keidel, S. Pöppl, Computer-aided detection of temporal patterns in human CNS dynamics, in: Progress in Computer-Assisted Function Analysis, Elsevier, Amsterdam, 1988, pp. 109–118.
[41] C.N. Byrns, M.W. Pitts, C.A. Gilman, A.C. Hashimoto, M.J. Berry, Mice lacking selenoprotein P and selenocysteine lyase exhibit severe neurological dysfunction, neurodegeneration, and audiogenic seizures, J. Biol. Chem. 289 (2014) 9662–9674, https://doi.org/10.1074/jbc.M113.540682.
[42] D.E. Fomenko, S.V. Novoselov, S.K. Natarajan, B.C. Lee, A. Koc, B.A. Carlson, T. H. Lee, H.Y. Kim, D.L. Hatfield, V.N. Gladyshev, MsrB1 (methionine-R-sulfoxide reductase 1) knock-out mice: roles of MsrB1 in redox regulation and identification of a novel selenoprotein form, J. Biol. Chem. 284 (2009) 5986–5993, https://doi.org/10.1074/jbc.M805770200.
[43] B.A. Carlson, U. Schweizer, C. Perella, R.K. Shrimali, L. Feigenbaum, L. Shen, S. Speransky, T. Floss, S.J. Jeong, J. Watts, V. Hoffmann, G.F. Combs, V. N. Gladyshev, D.L. Hatfield, The selenocysteine tRNA STAF-binding region is essential for adequate selenocysteine tRNA status, selenoprotein expression and early age survival of mice, Biochem. J. 418 (2009) 61–71, https://doi.org/10.1042/BJ20081304.
[44] J. Marksteiner, M. Ortler, R. Bellmann, G. Sperk, Neuropeptide Y biosynthesis is markedly induced in mossy fibers during temporal lobe epilepsy of the rat, Neurosci. Lett. 112 (1990) 143–148, https://doi.org/10.1016/0304-3940(90)90193-d.
[45] M.M. Peters, K.E. Hill, R.F. Burk, E.J. Weeber, Altered hippocampus synaptic function in selenoprotein P deficient mice, Mol. Neurodegener. 1 (2006) 12.
[46] J.W. Kinney, C.N. Davis, I. Tabarean, B. Conti, T. Bartfai, M.M. Behrens, A specific role for NR2A-containing NMDA receptors in the maintenance of parvalbumin and GAD67 immunoreactivity in cultured interneurons, J. Neurosci. 26 (2006) 1604–1615.
[47] O. Leiter, Z. Zhuo, R. Rust, J.M. Wasielewska, L. Grönnert, S. Kowal, R.W. Overall, V.S. Adusumilli, D.G. Blackmore, A. Southon, K. Ganio, C.A. McDevitt, N. Rund, D. Brici, I.A. Mudiyan, A.M. Sykes, A.E. Rünker, S. Zocher, S. Ayton, A.I. Bush, P. F. Bartlett, S.-T. Hou, G. Kempermann, T.L. Walker, Selenium mediates exercise-induced adult neurogenesis and reverses learning deficits induced by hippocampal injury and aging, Cell Metabol. 34 (2022) 408–423, https://doi.org/10.1016/j.cmet.2022.01.005, e8.
[48] J. Soerensen, C. Jakupoglu, H. Beck, H. Forster, J. Schmidt, W. Schmahl, U. Schweizer, M. Conrad, M. Brielmeier, The role of thioredoxin reductases in brain development, PLoS One 3 (2008), e1813, https://doi.org/10.1371/journal.pone.0001813.
[49] M. Christen, S. Hogler, M. Kleiter, M. Leschnik, C. Weber, D. Thaller, V. Jagannathan, T. Leeb, Deletion of the SELENOP gene leads to CNS atrophy with cerebellar ataxia in dogs, PLoS Genet. 17 (2021), e1009716, https://doi.org/10.1371/journal.pgen.1009716.
[50] O. Agamy, B. Ben Zeev, D. Lev, B. Marcus, D. Fine, D. Su, G. Narkis, R. Ofir, C. Hoffmann, E. Leshinsky-Silver, H. Flusser, S. Sivan, D. Soll, T. Lerman-Sagie, O. S. Birk, Mutations disrupting selenocysteine formation cause progressive cerebello-cerebral atrophy, Am. J. Hum. Genet. 87 (2010) 538–544.
[51] N. Fradejas-Villar, W. Zhao, U. Reuter, M. Doengi, I. Ingold, S. Bohleber, M. Conrad, U. Schweizer, Missense mutation in selenocysteine synthase causes cardio-respiratory failure and perinatal death in mice which can be compensated by selenium-independent GPX4, Redox Biol. 48 (2021), 102188, https://doi.org/10.1016/j.redox.2021.102188.
[52] I. Ingold, C. Berndt, S. Schmitt, S. Doll, G. Poschmann, K. Buday, A. Roveri, X. Peng, F. Porto Freitas, T. Seibt, L. Mehr, M. Aichler, A. Walch, D. Lamp, M. Jastroch, S. Miyamoto, W. Wurst, F. Ursini, E.S.J. Arner, N. Fradejas-Villar, U. Schweizer, H. Zischka, J.P. Friedmann Angeli, M. Conrad, Selenium utilization by GPX4 is required to prevent hydroperoxide-induced ferroptosis, Cell 172 (2018) 409–422, https://doi.org/10.1016/j.cell.2017.11.048, e21.
[53] H. Liu, F. Forouhar, T. Seibt, R. Saneto, K. Wigby, J. Friedman, X. Xia, M. S. Shchepinov, S.K. Ramesh, M. Conrad, B.R. Stockwell, Characterization of a patient-derived variant of GPX4 for precision therapy, Nat. Chem. Biol. 18 (2022) 91–100, https://doi.org/10.1038/s41589-021-00915-2.
[54] A.C. Smith, A.J. Mears, R. Bunker, A. Ahmed, M. MacKenzie, J. A. Schwartzentruber, C.L. Beaulieu, E. Ferretti, , Forge Canada Consortium, J. Majewski, D.E. Bulman, F.C. Celik, K.M. Boycott, G.E. Graham, Mutations in the enzyme glutathione peroxidase 4 cause Sedaghatian-type spondylometaphyseal dysplasia, J. Med. Genet. 51 (2014) 470–474, https://doi.org/10.1136/jmedgenet-2013-102218.
[55] A.P. Kudin, G. Baron, G. Zsurka, K.G. Hampel, C.E. Elger, A. Grote, Y. Weber, H. Lerche, H. Thiele, P. Nurnberg, H. Schulz, A.K. Ruppert, T. Sander, Q. Cheng, E. S. Arner, L. Schomburg, S. Seeher, N. Fradejas-Villar, U. Schweizer, W.S. Kunz, Homozygous mutation in TXNRD1 is associated with genetic generalized epilepsy, Free Radic. Biol. Med. 106 (2017) 270–277, https://doi.org/10.1016/j.freeradbiomed.2017.02.040.
[56] M.Y. Ahmed, A. Al-Khayat, F. Al-Murshedi, A. Al-Futaisi, B.A. Chioza, J. Pedro Fernandez-Murray, J.E. Self, C.G. Salter, G.V. Harlalka, L.E. Rawlins, S. Al-Zuhaibi, F. Al-Azri, F. Al-Rashdi, A. Cazenave-Gassiot, M.R. Wenk, F. Al-Salmi, M.A. Patton, D.L. Silver, E.L. Baple, C.R. McMaster, A.H. Crosby, A mutation of EPT1 (SELENOI) underlies a new disorder of Kennedy pathway phospholipid biosynthesis, Brain 140 (2017) 547–554, https://doi.org/10.1093/brain/aww318.
[57] Y. Horibata, O. Elpeleg, A. Eran, Y. Hirabayashi, D. Savitzki, G. Tal, H. Mandel, H. Sugimoto, EPT1 (selenoprotein I) is critical for the neural development and maintenance of plasmalogen in humans, J. Lipid Res. 59 (2018) 1015–1026, https://doi.org/10.1194/jlr.P081620.